

# UV-Stable Paper Coated with APTES-Modified P25 TiO<sub>2</sub> Nanoparticles

Fei Cheng, Seyed Mani Sajedin and Stephen M. Kelly\*

5 *Department of Chemistry, University of Hull, Cottingham Road, Hull, HU6 7RX, UK*

Adam F. Lee

10 *European Bioenergy Research Institute, Aston University, Aston Triangle, Birmingham, B4  
7ET, UK*

Andreas Kornherr

15 *Mondi Uncoated Fine Paper, Haidmuehlstrasse 2-4, A-3363 Ulmerfeld-Hausmening, Austria*

## Abstract

In order to inhibit the photocatalytic degradation of organic material supports induced by small titania (TiO<sub>2</sub>) nanoparticles, highly photocatalytically active, commercially available  
20 P25-TiO<sub>2</sub> nanoparticles were first modified with a thin layer of (3-aminopropyl)triethoxysilane (APTES), which were then deposited *and* fixed onto the surface of paper samples *via* a simple, dip-coating process in water at room temperature. The resultant APTES-modified P25 TiO<sub>2</sub> nanoparticle-coated paper samples exhibit much greater stability to UV-illumination than uncoated blank reference paper. Very little, or no, photo-  
25 degradation in terms of brightness and whiteness, respectively, of the P25-TiO<sub>2</sub>-nanoparticle-treated paper is observed. There are many other potential applications for this Green Chemistry approach to protect cellulosic fibres from UV-bleaching in sunlight and to protect their whiteness and maintain their brightness.

30 \*Corresponding author: Tel: +44 1482 466347; *E-mail*: [s.m.kelly@hull.ac.uk](mailto:s.m.kelly@hull.ac.uk)

Keywords: P25 TiO<sub>2</sub> nanoparticles, APTES, UV-stable paper, dip-coating, green chemistry

## 1 Introduction

35 Titanium dioxide (TiO<sub>2</sub>) is a very important industrial material. It has been widely used, for example, in pigments, paints, cosmetics, photocatalysis and photocatalyst supports. (Chen, Wang, & Chiu, 2007; Gesenhues, 2001; Fernandez-Garcia, Martinez-Arias,

Hanson, & Rodriguez, 2004; Hebeish, Abdelhady, & Youssef, 2013; Youssef, Kamel, & El-Samahy, 2013) Titanium dioxide has also been used for anti-reflection and optical coatings as well as beam splitters due to its large dielectric constant and high refractive index. (Samuel, Pasricha, & Ravi, 2005) Titanium dioxide naturally exists in three crystalline polymorphs, i.e., anatase, rutile and brookite of which the most commonly used forms are anatase and rutile. (Pelton, Geng, & Brook, 2006; Wold, 1993) Both the anatase and rutile TiO<sub>2</sub> polymorphs are in photocatalysis, for example, whereby the anatase TiO<sub>2</sub> polymorph shows the higher photocatalytic activity. (Linsebigler, Lu, & Yates, 1995) P25 is a commercial TiO<sub>2</sub> powder (EVONIK), which consists of 80% of the anatase phase and 20% of the rutile phase of titanium dioxide. These commercial titania nanoparticles have been widely used as photocatalysts in photochemical reactions due to their very high photocatalytic activity. (Ryu, & Choi, 2008) Unfortunately, the high redox activity of titania can lead to photodegradation of any organic substrate, support, functional material, etc., which limits the application of titania nanoparticles in the paper, textile, paint and plastic film industries, for example. The use of rutile titania nanoparticles with a large diameter ( $d > 200$  nm), and core/shell TiO<sub>2</sub>/SiO<sub>2</sub> nanoparticles are the most common approaches adopted to inhibit the photocatalytic effect of TiO<sub>2</sub> nanoparticles and thereby to inhibit the degradation of the catalyst support. (Furusawa, Honda, Ukaji, Sato, & Suzuki, 2008)

3-Aminopropyltriethoxysilane (APTES) is frequently used as a coupling agent for attaching organic molecules to hydroxylated silicon oxide or metal oxide substrates, due to the presence of the terminal amine group on the propyl chain, (Kim, Cho, Seidler, Kurland, & Yadavalli, 2010; Pasternack, Amy, & Chabal, 2008) for example, APTES has been used to link proteins to TiO<sub>2</sub> surfaces or to promote cell adhesion to TiO<sub>2</sub> surfaces. (Balasundaram, Sato, & Webster, 2006; Filippini, Rainaldi, Ferrante, Mecheri, Gabrielli, Bombace, Indovina, & Santini, 2001) Adsorption of APTES-modified organic dyes onto TiO<sub>2</sub> surfaces has also been reported using APTES as the coupling agent. (Andrzejewska, Krysztalkiewicz, & Jesionowski, 2004) Although in many cases APTES has been used for many applications, the nature of the dominant conformation or chemical form of APTES at interfaces is often open to doubt and conjecture, because these factors depend not only on the reaction conditions, but also on the crystal structure of the TiO<sub>2</sub> substrate. (Song, Hildebrand, & Schmuki, 2010; Chen, & Yakovlev, 2010; Ukaji, Furusawa, Sato, & Suzuki, 2007) APTES has not, to the authors' best knowledge, been used so far to deposit and bind TiO<sub>2</sub> nanoparticles to the surface of cellulose or to that of its many diverse derivatives.

Cellulose is the most abundant, widespread and naturally occurring biopolymer in nature. Alongside its traditional applications in paper and cotton textiles, cellulose is also a very important environmentally friendly, biocompatible and cost-effective, carbon-based resource for the development of novel advanced functional materials. (Habibi, Lucia, & Rojas, 2010) Cellulose is a high-molecular-weight, linear, mainchain carbohydrate polymer consisting of repeating  $\beta$ -D-glucopyranose moieties, which are linked covalently through acetal functions between the equatorial OH groups. The presence of a large number of hydrophilic hydroxyl groups (Klemm, Heublein, Fink, & Bohn, 2005; Roy, Semsarilar, Guthrie, & Perrier, 2009) in cellulose and its derivatives can promote the nucleation and growth of inorganic phases at the cellulose fibre surface and thus facilitate the production of organic/inorganic nanocomposites. (Pinto, Marques, Barros-Timmons, Trindade, & Neto, 2008; Li, Chen, Hu, Shi, Shen, Zhang, & Wang, 2009; Iguchi, Ichiura, Kitaoka, & Tanaka, 2003)

The protection of cellulosic textiles against different kinds of degradation and the creation of new functionalised cellulose derivatives can be realised by coating the textiles with silica sols with a nanoparticle diameter smaller than 50 nm. (Mahltig, Haufe, & Bottcher, 2005). The surface of vegetable cellulose fibres has been modified, for example, with a nanoparticle-functionalised siloxane coating, first using the hydrolysis of tetraethoxysilane (TEOS), octyltrimethoxysilane (OTMS) or polydimethylsiloxane (PTMS), followed then by layer-by-layer deposition of previously synthesized titanium dioxide nanoparticles. (Goncalves, Marques, Pinto, Trindade, & Neto, 2009) Morphologically well-defined silica nanoparticles have been successfully deposited onto cellulose fibre surfaces *via* a polyelectrolytes layer-by-layer approach. (Pinto, Marques, Barros-Timmons, Trindade, & Neto, 2008)

In this report, commercially available, highly photochemically active and strongly UV-absorbing P25 TiO<sub>2</sub> nanoparticles (EVONIK) have been modified to form a strongly UV-absorbing, but non-photo-catalytically active, coating on the surface of cellulose paper in order to significantly improve its resistance to UV-degradation in terms of maintaining the original brightness and whiteness of paper samples under standard, commercial UV-illumination test conditions. In a simple, two-step process, the surface of small, photo-active titania nanoparticles was first modified with a thin coating of APTES to produce deactivated, APTES-coated TiO<sub>2</sub> nanoparticles, which were then deposited *and* fixed on the surface of paper simply using a very simple, water-based dip-coating procedure at room temperature.,

The APTES-modified TiO<sub>2</sub> nanoparticles protect the paper from photochemical bleaching as far as possible under standard UV-illumination test conditions. No impact or spray coating techniques, chemical binders, surfactants, dispersants or a post-treatment curing step are required in this two-step process. The presence of additional amine and silane groups present in the APTES coating covering the surface of the APTES-modified TiO<sub>2</sub> nanoparticles should promote attachment *and* fixation to the many hydroxyl-groups present on the surface of the cellulose fibres. The APTES-modified TiO<sub>2</sub> nanoparticles are prepared in a simple fashion at a relatively low reaction temperature. The structural and mechanical properties of the cellulose fibres will not be impaired by the presence of the APTES-modified TiO<sub>2</sub> nanoparticles, whose presence just on the outer surface, not in the core, of the fibre will ensure a high effective absorption of UV-light. A much lower loading of nanoparticles is required using this surface-based approach than dispersing nanoparticles in the bulk fibre mixtures used to prepare paper, fabrics, textiles, etc., which is advantageous in terms of minimising contamination of the environment with nanoparticles.

15

## 2 Experimental

### 2.1 Materials and characterization methods

The TiO<sub>2</sub> P25 nanoparticles were sourced from EVONIK. (3-Aminopropyl)triethoxysilane [APTES, (C<sub>2</sub>H<sub>5</sub>O)<sub>3</sub>Si(CH<sub>2</sub>)<sub>3</sub>NH<sub>2</sub>] and xylene were supplied by Aldrich and used as received. The paper samples, which are 1 mm thick and which do not possess a surface coating, such calcium carbonate or china clay, were provided by Mondi Uncoated Fine Paper, Austria. Acetone was sourced from Fisher Scientific, UK, and used as received.

Fourier transform infrared spectra were recorded on a Nicolet Magna-500 FTIR spectrometer. X-ray powder diffraction (XRD) analyses were performed on a SIEMENS D5000 Instrument. Scanning electron microscopy (SEM) images were obtained using a Carl Zeiss SMT 'EVO60' SEM microscope operating at 20 kV and EDX data were obtained using an Oxford Instruments 'INCA' Energy Dispersive X-ray Spectrometer. Transmission electron microscopy (TEM) was collected using a Jeol 2010 TEM running at 200kV. TEM images were obtained with a Gatan Ultrascan 4000 digital camera. Solid samples were prepared by suspension in distilled water and 5 µl aliquots of a suitable dilution dropped onto carbon-coated copper grids. The BET surface area and pore size diameter of the various titania

30

powders were calculated from nitrogen adsorption/desorption isotherms at 77 K using a Micromeritics three star 3000 instrument. The whiteness of the standard paper samples and the APTES-modified TiO<sub>2</sub> nanoparticle paper samples was measured using a standard whiteness tester (Lorentzen&Wettre, Elrepho). The brightness of these samples was determined, before and after the suntest (Suntest XLS+; ATLAS Material Testing Solutions). The suntester allows irradiation of paper samples with a xenon lamp under accurate, repeatable conditions (i.e. 90 min, 500 W, and 2700 kJ/m<sup>2</sup>). XPS was performed on a Kratos Axis HSi X-ray photoelectron spectrometer fitted with a charge neutraliser and magnetic focusing lens employing Al K<sub>α</sub> monochromatic radiation (1486.7 eV). Surface elemental analysis was undertaken on Shirley background-subtracted spectra applying the appropriate instrument- and element-specific response factors. Spectral fitting was conducted using CasaXPS, version 2.3.14, with binding energies corrected to the C 1s peak at 284.5 eV and with the high-resolution C 1s, O 1s, N 1s, Si 2p and Ti 2p XP spectra fitted using a common Gaussian/Lorentzian peak shape. Errors were estimated by varying the Shirley background subtraction procedure across reasonable limits and re-calculating fits. The photocatalytic activity of the P25 TiO<sub>2</sub> and APTES-modified TiO<sub>2</sub> was evaluated in terms of the degradation of Rhodamine B. (Ren, Chen, Zhang, & Wu, 2010) P25 TiO<sub>2</sub> or APTES-modified TiO<sub>2</sub>-powder (10 mg) was suspended in 10 mL of water and then 10 mL of Rhodamine B solution (20 mg/L) was added to the suspension solution. The UV irradiation was carried out under a UV light at 365 nm for 30 min. The suspension solutions were centrifuged at 10000 rpm for 15 min. The Rhodamine B content in the solutions was determined by UV-Vis analysis in the range between 300 and 700 nm using a Perkin Elmer Lambda 25 spectrometer.

## 2.2 Modification of TiO<sub>2</sub> surfaces with APTES (TiO<sub>2</sub>-APTES)

APTES (1.5 mL) was added to a stirred suspension of P25 TiO<sub>2</sub> nanoparticles (0.5 g) in xylene (50 mL). After allowing the reaction mixture to react at 50 °C for 10 h, a white powder was obtained by centrifugation of the cooled reaction mixture, which was then washed with xylene and then twice with acetone followed by drying under vacuum overnight.

### 2.3 Coating of papers with APTES modified TiO<sub>2</sub> nanoparticles

The APTES-stabilised P25 TiO<sub>2</sub> nanoparticle powder was added to distilled water (20mL) and sonicated for 15 min to produce a stable, aqueous colloidal solution of APTES-stabilised P25 TiO<sub>2</sub> nanoparticles. A sample of commercial uncoated paper (0.7 g) was then immersed in the aqueous colloidal solution. After sonication for 15 min, the paper sample, now coated with APTES-stabilised P25 TiO<sub>2</sub> nanoparticles, was washed carefully with copious amounts of distilled water and dried under vacuum overnight.

## 3 Results and Discussions

### 3.1 Modification of P25 TiO<sub>2</sub> nanoparticles with APTES

The IR spectra of the P25 TiO<sub>2</sub> nanoparticles and APTES-modified P25 TiO<sub>2</sub> nanoparticles shown in Fig. 1 reveal a small peak at 1640 cm<sup>-1</sup> and large, broad peak between 3450 and 3200 cm<sup>-1</sup>, which are due to stretching vibrations of absorbed water, as well as surface hydroxyl (-OH) groups present on the surface of the nanopowder. (Chen, & Yakovlev, 2010) The broad peak between 600–400 cm<sup>-1</sup> can be confidently assigned to the presence of Ti–O–Ti bonds. Compared with the P25 TiO<sub>2</sub> nanoparticles, the APTES-modified P25 TiO<sub>2</sub> nanoparticles show an additional weak band at 2923 cm<sup>-1</sup>, which can be assigned to the alkyl groups [-(CH<sub>2</sub>)<sub>n</sub>-] present in APTES. The new absorption band at 1561 cm<sup>-1</sup> is attributable to a NH<sub>2</sub> scissor vibration, suggesting the presence of the amino groups of APTES molecules in the terminal position of the propyl chain. (Pasternack, Amy, & Chabal, 2008) Furthermore, the peak at around 1024 cm<sup>-1</sup> can be assigned to the stretch vibration of Ti–O–Si moieties, formed by a condensation reaction between silanol groups of the APTES and hydroxyl groups present on the surface TiO<sub>2</sub> nanoparticles. (Ukaji, Furusawa, Sato, & Suzuki, 2007) In addition, the broad band at around 1116 cm<sup>-1</sup> is probably attributable to the stretch vibration of Si–O–Si, produced by the condensation reactions between silanol groups. (Chen, & Yakovlev, 2010) All these facts suggest that APTES has been successfully attached as a thin film to the surface of the P25 TiO<sub>2</sub> nanoparticles.

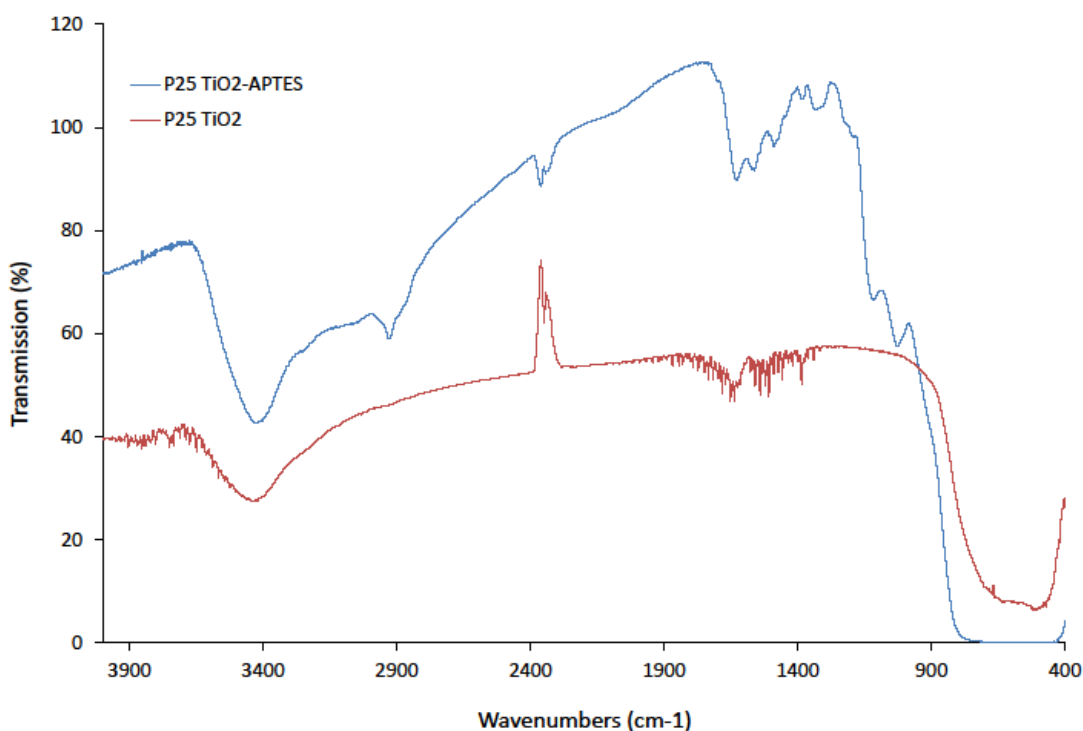


**Fig. 1.** Infrared spectra of commercially available P25 TiO<sub>2</sub> nanoparticles and APTES-modified P25 TiO<sub>2</sub> nanoparticles.

5           The XPS spectra of the P25 TiO<sub>2</sub> nanoparticles and those of the corresponding APTES-modified P25 TiO<sub>2</sub> nanoparticles are shown in Fig. 2. In comparison with the survey spectrum of the P25 TiO<sub>2</sub> nanoparticles (Figure 2A), the APTES-modified P25 TiO<sub>2</sub> nanoparticles exhibit new peaks corresponding to N 1s and Si 2p photoemission features, clearly indicating successful modification of the titanium oxide surface by aminosilane

10           moieties. Fig. 2B-2F shows the corresponding, high-resolution C 1s, O 1s, Si 2p, N 1s and Ti 2p XP spectra. The C 1s spectra were deconvoluted using three components, C1, C2 and C3. The C1, C2 and C3 peaks in the C 1s spectrum of P25 TiO<sub>2</sub> nanoparticles at 284.41 (82.7 %), 286.04 (9.44 %) and 288.15 (7.86 %) (Table 1) are assigned to CH<sub>x</sub>, C-O and C=O bonds respectively, associated with the presence of hydrocarbon impurities resulting from sample

15           preparation and handling. (Arranz, Palacio, Garcia-Fresnadillo, Orellana, Navarro, & Munoz, 2008) APTES-modified titania nanoparticles also exhibit three carbon components at 284.84 (68.33 %), 286.20 (18.51 %) and 288.16 (13.17 %), which are attributed to the presence of CH<sub>x</sub>/C-C/C-Si, C-N/C-O and C=O functions, respectively. (Song, Hildebrand, & Schmuki, 2010) The C3 component likely arises from organic residues incorporated during sample

20           handing/transportation, since APTES does not contain a carbonyl function. Such high-

binding-energy carbon moieties have also been reported during the APTES modification of GaN and amorphous TiO<sub>2</sub> surfaces. (Song, Hildebrand, & Schmuki, 2010; Song, Hildebrand, & Schmuki, 2010) The O 1s spectrum also exhibits a new peak at 532.13 eV after APTES modification, ascribed here to the presence of O-Si-R surface species. The presence of a sharp peak at 102.13 eV in the Si 2p provides clear evidence of the successful attachment of APTES to the surface of the TiO<sub>2</sub> nanoparticles, with surface compositional analysis showing that the APTES-modified titania possesses 17.2 atom% silicon (Table 2). Three new N 1s peaks were also observed following APTES-modification at 339.18, 400.61 and 401.61 eV. The 339.18 eV component is assigned to the presence of the terminal NH<sub>2</sub> groups in the APTES coating on the surface of the P25 TiO<sub>2</sub> nanoparticles, whereas the peaks at 400.61 and 401.61 eV are possibly due to hydrogen-bonded amino (-NH<sub>2</sub>) or protonated amino-groups (-NH<sub>3</sub><sup>+</sup>). (Song, Hildebrand, & Schmuki, 2010)

The possible modes of interactions of APTES, which has two distinct terminal functional groups, i.e., the hydrolysable silane, -Si(OR)<sub>3</sub>, group and the amino- (-NH<sub>2</sub>) group, with the TiO<sub>2</sub> nanoparticle surface are shown in Fig. 3. (Ukaji, Furusawa, Sato, & Suzuki, 2007; Acres, Ellis, Alvino, Lenahan, Khodakov, Metha, & Andersson, 2012) If the silane groups react with hydroxyl groups present on the TiO<sub>2</sub> nanoparticle surface to form a silanized surface, as shown in Fig. 3a-d, then free terminal -NH<sub>2</sub> groups, which project away from the TiO<sub>2</sub> nanoparticle surface, can be observed at 399.18 eV (normal attachment). On the other hand, if the -NH<sub>2</sub> groups are attached to the surface through hydrogen bonding, or protonated amine (-NH<sub>3</sub><sup>+</sup>), then ionic bonding, with the hydroxyl groups present on the TiO<sub>2</sub> nanoparticle surface, as shown in Fig. 3 (e) and 3(f), the N 1s peak will appear at higher energy (~ 400.9 eV), i.e., reverse attachment. Since the contribution of the peak at 399.18 eV is 60.42 % and, therefore, much higher than that of the peaks at 400.61 eV (24.92 eV) and 401.61 (14.67 eV), APTES appears to be mainly attached by silanized bonding with free terminal amino-groups projecting away from the nanoparticle surface, which would be similar to previously reported behaviour. (Pasternack, Amy, & Chabal, 2008; Arranz, Palacio, Garcia-Fresnadillo, Orellana, Navarro, & Munoz, 2008; Vandenberg, Bertilsson, Liedberg, Uvdal, Erlandsson, Elwing, & Lundstrom, 1991)

30

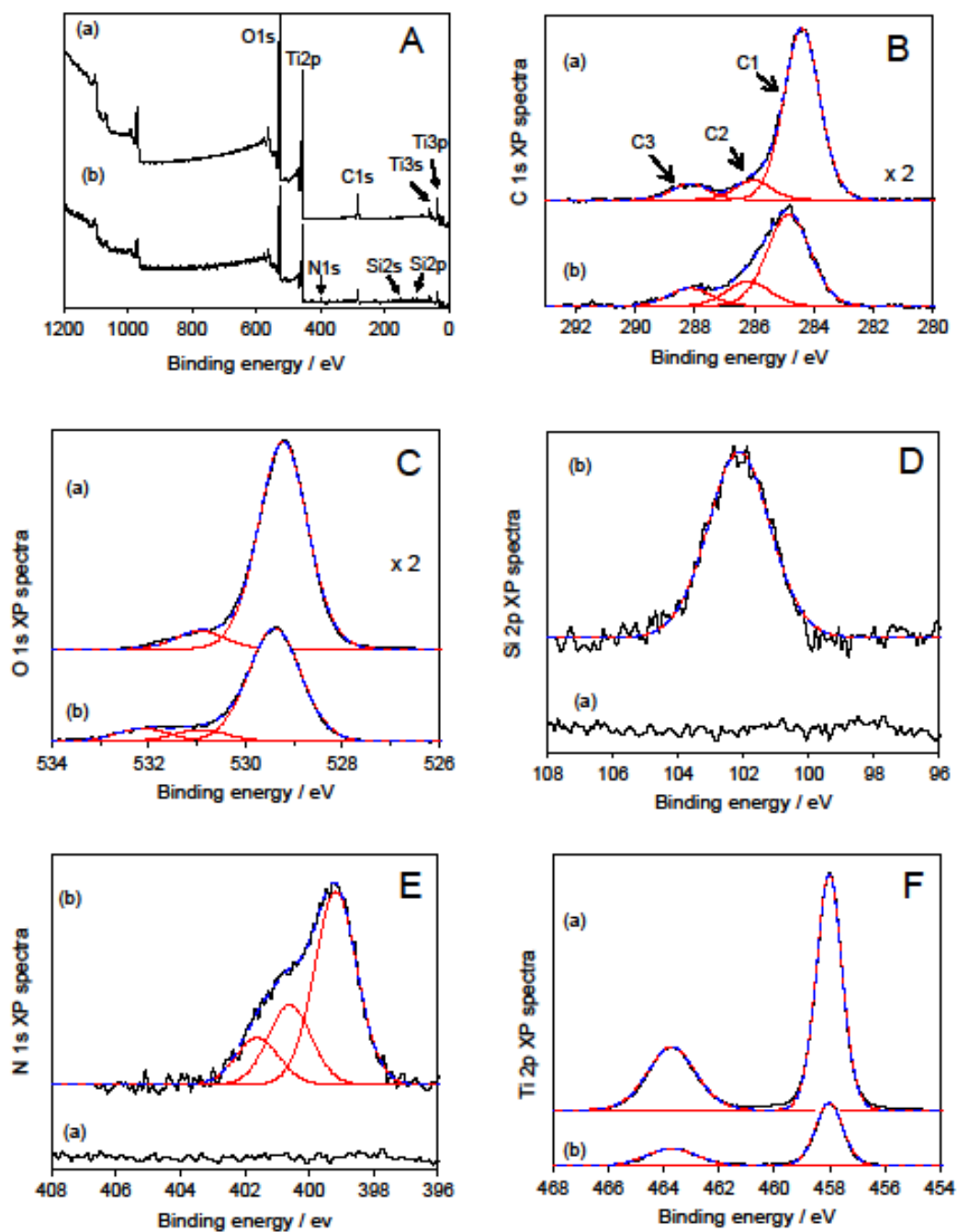


**Fig. 2.** (A) XPS survey spectra and (B) C 1s, (C) O 1s, (D) Si 2p, (E) N 1s and (F) Ti 2p high-resolution spectra of (a) commercially available, untreated P25 TiO<sub>2</sub> nanoparticles and (b) APTES-modified P25 TiO<sub>2</sub> nanoparticles.

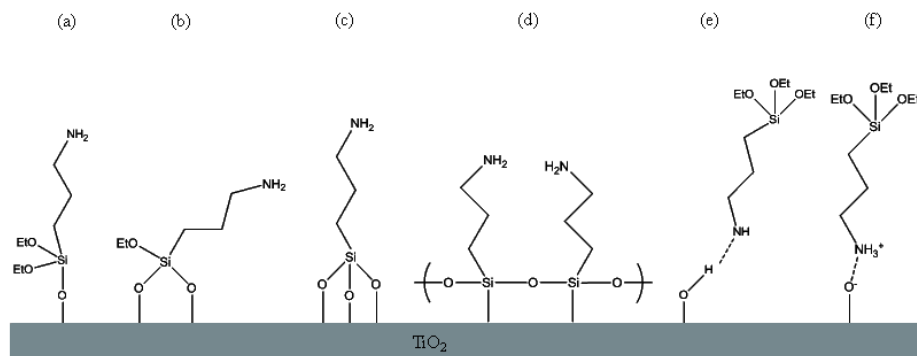
**Table 1** XPS surface analysis of P25 TiO<sub>2</sub> nanoparticles and APTES-modified TiO<sub>2</sub> nanoparticles

	TiO <sub>2</sub>		TiO <sub>2</sub> – APTES	
	Binding energy /eV	%	Binding energy /eV	%
Ti 2p	458.00		458.00	
O 1s	529.23	92.01	529.40	82.03
	530.94	7.99	530.93	8.63
			532.13	9.34
C 1s	284.41	82.70	284.84	68.33
	286.04	9.44	286.20	18.51
	288.15	7.86	288.16	13.17
N 1s			399.18	60.42
			400.61	24.92
			401.61	14.67
Si			102.13	

5

**Table 2** XPS surface elemental analysis for APTES-modified P25 TiO<sub>2</sub> nanoparticles.

Element	%
Ti	18.88
O	51.14
C	23.16
N	3.56
Si	3.25



10

**Fig. 3.** Possible surface interactions and potential modes of chemical bonding between a TiO<sub>2</sub> nanoparticle surface and (3-aminopropyl)triethoxysilane (APTES).

The active surface area of the APTES-modified P25 TiO<sub>2</sub> nanoparticles, as determined using a combination of absorption experiments and BET analysis, is 47.5 m<sup>2</sup>/g, which is marginally lower (2.5 m<sup>2</sup>/g) than that of the untreated P25 TiO<sub>2</sub> nanoparticles (50.0 m<sup>2</sup>/g), due to the coating of APTES on the surface of P25 TiO<sub>2</sub> nanoparticle powder. The photocatalytic activity of the P25 TiO<sub>2</sub> and that of the APTES-modified TiO<sub>2</sub> powders was tested by adding samples of the untreated and treated P25 TiO<sub>2</sub> nanoparticles to a Rhodamine solution followed by UV-irradiation of the resultant solutions at 365 nm for 30 min. The UV/vis analysis shows that 51.8% of Rhodamine is degraded by the APTES-modified P25 TiO<sub>2</sub> nanoparticles, compared with 58.5% of Rhodamine degradation by the untreated P25 TiO<sub>2</sub> nanoparticles (Fig. 4). The lower photocatalytic activity of APTES-modified P25 TiO<sub>2</sub> nanoparticles further supports the assumption that the surfaces of the APTES-treated P25 TiO<sub>2</sub> nanoparticles have indeed been coated with a monolayer of APTES. Furthermore, the TEM images of P25 TiO<sub>2</sub> and APTES APTES-modified P25 TiO<sub>2</sub> nanoparticles show no significant differences in size or shape of the nanoparticles before and after treatment (not shown), which indicates that the APTES-coating present on the TiO<sub>2</sub> surface is very thin, as could be reasonably expected.

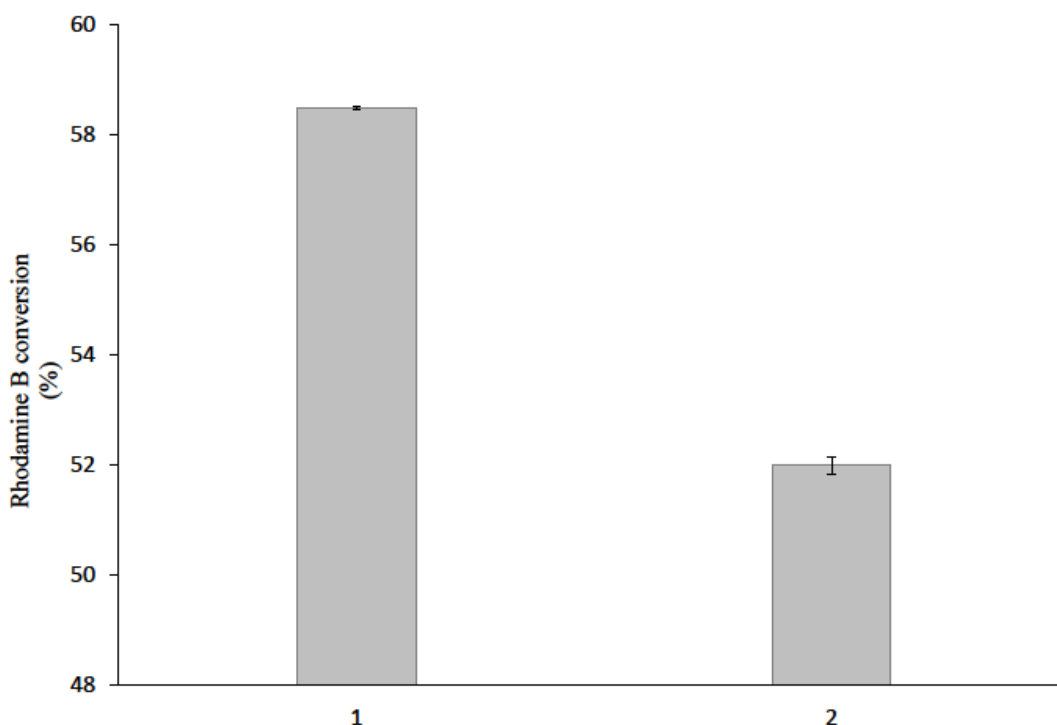
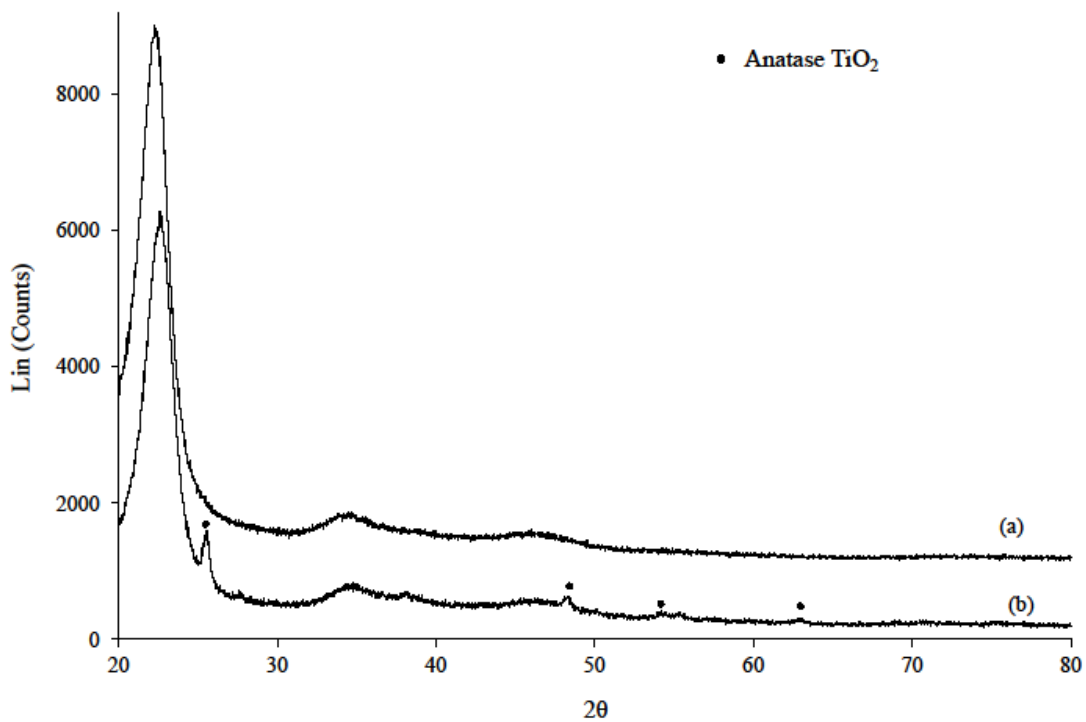


**Fig. 4.** The photodegradation of Rhodamine B induced by (1) commercially available P25 TiO<sub>2</sub> nanoparticles and (2) APTES-modified P25 TiO<sub>2</sub> nanoparticles, after 30 min of UV-irradiation

### 3.2 Deposition of APTES-modified P25 TiO<sub>2</sub> nanoparticles on paper

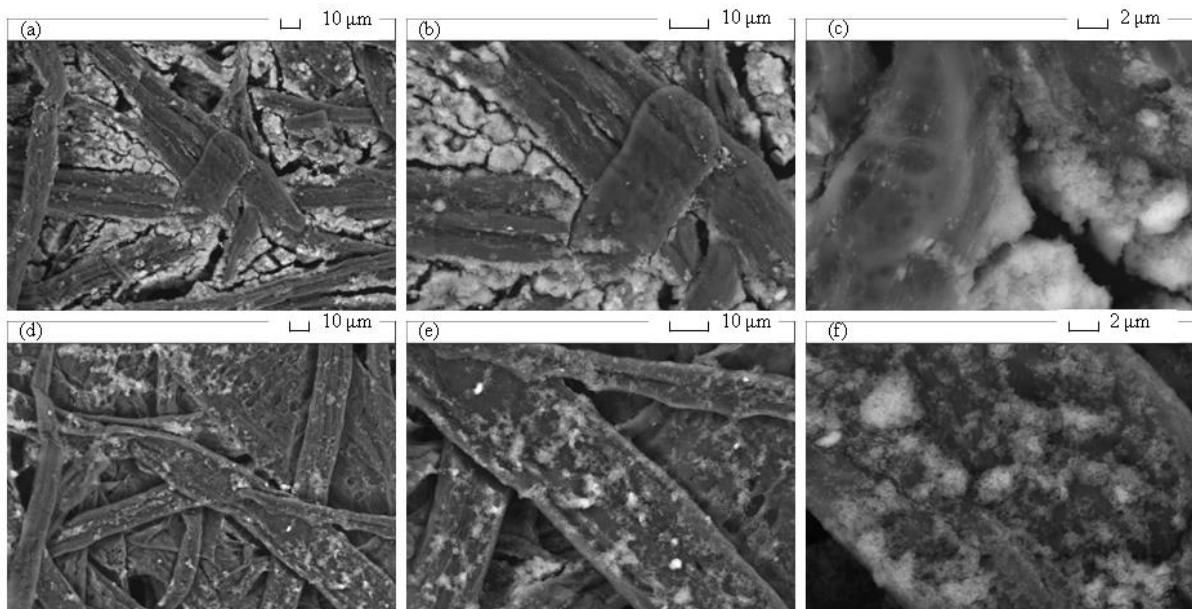
The APTES-modified P25 TiO<sub>2</sub> nanoparticles have free terminal amino-groups (attachment of -NH<sub>2</sub> groups normal to the surface) and hydrolysable silane groups (reverse attachment of -Si(OR)<sub>3</sub> groups). Therefore, the presence of free terminal amino groups can facilitate the attachment of the APTES-modified P25 TiO<sub>2</sub> nanoparticles to the cellulose fibres through hydrogen bonding between amino-, or protonated amino- (-NH<sub>3</sub><sup>+</sup>), groups with hydroxyl groups present on the surface on the surface of the cellulose fibres. The silane groups will also react with the hydroxyl groups on cellulose fibres to fix P25 TiO<sub>2</sub> nanoparticles irreversibly onto the surface of the cellulose paper. These hydrogen bonding interactions and chemical reactions ensure the irreversible fixation of the APTES-modified P25 TiO<sub>2</sub> nanoparticles onto the surface of the cellulose fibres. This thin layer of P25 TiO<sub>2</sub> nanoparticles cannot then removed by repeated washing with copious amounts of water.

Figure 5 shows the XRD patterns of the paper substrate and the paper coated with the APTES-modified P25 TiO<sub>2</sub> nanoparticles. It can be seen that beside a strong peak attributable to cellulose at  $2\theta = 23^\circ$ , a weak anatase titania peak, attributable to TiO<sub>2</sub>-P25, can also be observed. However, peaks attributable to the minority rutile polymorph, present in the standard, commercially available P25 TiO<sub>2</sub> nanoparticles, are probably too weak to be observed. SEM images also show that the surfaces of the cellulose fibres are covered with a thin coating of APTES-modified P25 TiO<sub>2</sub> nanoparticles and that no nanoparticles can be observed between the fibres of cellulose, see Fig. 6. In contrast, the untreated P25 TiO<sub>2</sub> nanoparticles are mainly located between the fibres of the cellulose, rather than being attached to the surface of the fibres themselves (Fig. 6).



**Fig. 5.** XRD pattern of (a) cellulose paper and (b) cellulose paper coated with APTES-modified P25 TiO<sub>2</sub> nanoparticles.

5



**Fig. 6.** SEM images of cellulose paper samples coated with (a, b and c) commercially available P25 TiO<sub>2</sub> nanoparticles and (d, e and f) APTES-modified P25 TiO<sub>2</sub> nanoparticles.

10

The ISO-brightness determined for the blank reference paper and the paper samples coated either with untreated P25 TiO<sub>2</sub> nanoparticles or APTES-modified P25 TiO<sub>2</sub> nanoparticles, before and after illumination with UV-light in the standard xenon UV-stability test, is shown in Fig. 7(a). It can be seen that the brightness of the blank paper reference is sharply reduced after illumination with UV radiation in the standard xenon test. The reduction in brightness is even more significant for the paper samples coated with untreated P25 TiO<sub>2</sub> nanoparticles. In contrast, there is only a marginal reduction in the brightness of the paper samples coated with APTES-modified P25 TiO<sub>2</sub> nanoparticles. It seems reasonable to assume that the small reduction in the brightness of the APTES-modified P25 TiO<sub>2</sub> nanoparticle coated paper sample, after the xenon UV-test, is attributable to the fact that the photo-catalytically active titania nanoparticles have been coated effectively with a thin, inert layer of APTES, which passivates their surface and thereby inhibits their inherent photocatalytic activity. The value for the CIE-whiteness of the cellulose paper coated with APTES-modified P25 TiO<sub>2</sub> nanoparticles is slightly higher than that of either the blank paper reference and that of the P25 TiO<sub>2</sub>-nanoparticle-coated paper sample, see Fig. 7(b). In contrast to the sharp reduction in the whiteness of the blank paper reference sample and the P25 TiO<sub>2</sub> nanoparticle coated paper sample, no reduction in whiteness can be observed for the paper coated with the APTES-modified P25 TiO<sub>2</sub> nanoparticles, after the standard xenon UV-stability test.

20

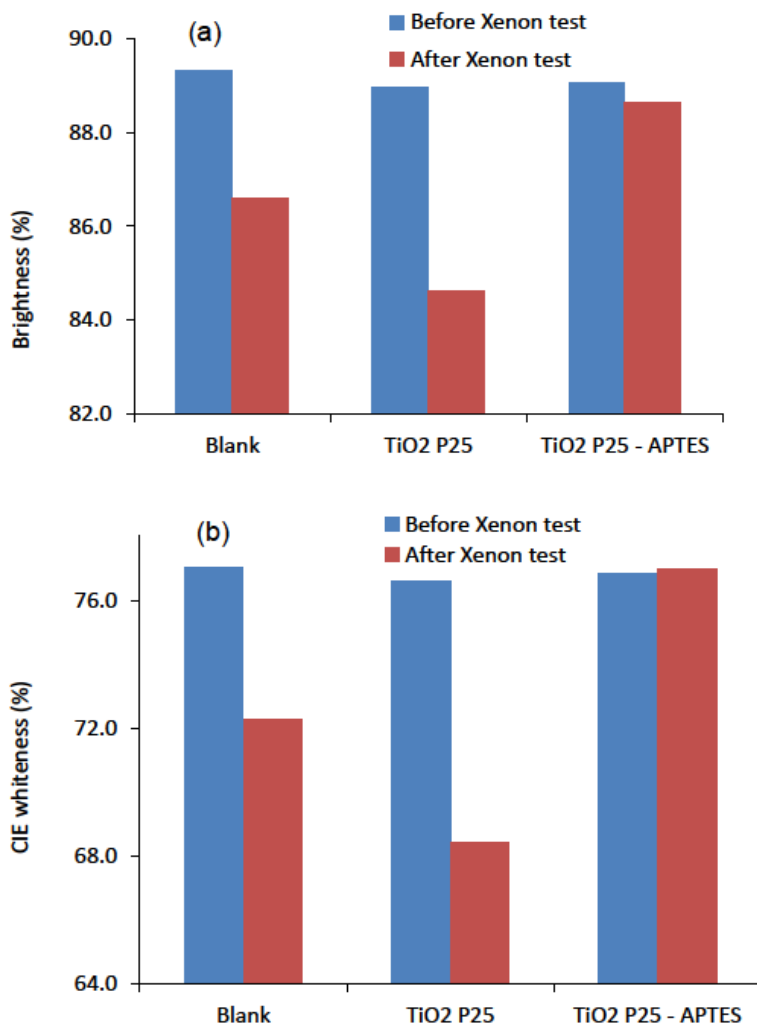


**Fig. 7.** (a) ISO-brightness and (b) CIE whiteness of blank reference paper and the paper samples coated either with untreated P25 TiO<sub>2</sub> nanoparticles or APTES-modified P25 TiO<sub>2</sub> nanoparticles before and after the UV-stability test.

5

### 3.3 Conclusion

A simple dip-coating procedure has been successfully applied to attach APTES-modified, commercially available P25 TiO<sub>2</sub> nanoparticles onto the surface of standard, commercial uncoated paper samples. The presence of free terminal NH<sub>2</sub> groups and hydrolysable silane groups in the APTES-modified P25 TiO<sub>2</sub> nanoparticles contributes to the attachment of TiO<sub>2</sub> onto the surface of the constituent fibres of the paper samples. The presence of the APTES coating between the titania nanoparticles and cellulose fibres effectively inhibits the strong photocatalytic degradation effect of the titania nanoparticles. The paper samples coated with APTES-modified P25 TiO<sub>2</sub> nanoparticles exhibit a significantly higher stability to UV-bleaching than that of the untreated commercial paper reference.

## Acknowledgements

We thank the European Union Seventh Framework Programme (FP7/2007-2013) for financial support under Grant Agreement Number 214653 (SURFUNCELL project), and the  
5 EPSRC for the award of a Leadership Fellowship (EP/G007594/3) to AFL. Mrs A Lowry, Mr A Sinclair, Mr R Knight and Mr M. Isaacs are thanked for providing TEM, SEM, ICP and XPS analyses, respectively.

## References

- 10  
Acres, R. G., Ellis, A. V., Alvino, J., Lenahan, C. E., Khodakov, D. A., Metha, G. F., & Andersson, G. G.(2012). Molecular Structure of 3-Aminopropyltriethoxysilane Layers Formed on Silanol-Terminated Silicon Surfaces. *Journal of Physical Chemistry C*, *116*(10), 6289-6297.
- 15 Andrzejewska, A., Krysztafkiewicz, A. & Jesionowski, T. (2004). Adsorption of organic dyes on the aminosilane modified TiO<sub>2</sub> surface. *Dyes and Pigments*, *62*(2), 121-130.
- Arranz, A., Palacio, C., Garcia-Fresnadillo, D., Orellana, G., Navarro, A., & Munoz, E.(2008). Influence of surface hydroxylation on 3-aminopropyltriethoxysilane growth  
20 mode during chemical functionalization of GaN surfaces: An angle-resolved X-ray photoelectron spectroscopy study. *Langmuir*, *24*(16), 8667-8671.
- Balasundaram, G., Sato, M., & Webster, T. J. (2006). Using hydroxyapatite nanoparticles and decreased crystallinity to promote osteoblast adhesion similar to functionalizing with RGD. *Biomaterials*, *27*(14), 2798-2805.
- 25 Chen, H.J., Wang, L., & Chiu, W.Y. (2007). Chelation and solvent effect on the preparation of titania colloids. *Materials Chemistry and Physics*, *101*(1), 12-19.
- Chen, Q., & Yakovlev, N. L. (2010) Adsorption and interaction of organosilanes on TiO<sub>2</sub> nanoparticles. *Applied Surface Science*, *257*(5), 1395-1400.
- Fernandez-Garcia, M., Martinez-Arias, A., Hanson, J. C., & Rodriguez, J. A.  
30 (2004). *Nanostructured oxides in chemistry: Characterization and properties. Chemical Reviews*, *104*(9), 4063-4104.
- Filippini, P., Rainaldi, C., Ferrante, A., Mecheri, B., Gabrielli, G., Bombace, M.,

- Indovina, P. L., & Santini, M. T. (2001). Modulation of osteosarcoma cell growth and differentiation by silane-modified surfaces. *Journal of Biomedical Materials Research*, 55(3), 338-349.
- 5 Furusawa, T., Honda, K., Ukaji, E., Sato, M., & Suzuki, N. (2008). The microwave effect on the properties of silica-coated TiO<sub>2</sub> fine particles prepared using sol-gel method. *Materials Research Bulletin*, 43(4), 946-957.
- Gesenhues, U. (2001). Calcination of metatitanic acid to titanium dioxide white pigments. *Chemical Engineering & Technology*, 24(7), 685-694.
- 10 Goncalves, G., Marques, P., Pinto, R. J. B., Trindade, T., & Neto, C. P. (2009). Surface modification of cellulosic fibres for multi-purpose TiO<sub>2</sub> based nanocomposites. *Composites Science and Technology*, 69(7-8), 1051-1056.
- Habibi, Y., Lucia, L.A., & Rojas, O. J. (2010). Cellulose nanocrystals: chemistry, self-assembly, and applications. *Chemical Reviews*, 110(6), 3479-3500.
- 15 Hebeish A. A., Abdelhady M. M., & Youssef A. M. (2013). TiO<sub>2</sub> nanowires and TiO<sub>2</sub> nanowires doped Ag- PVP nanocomposites for antimicrobial and self-cleaning cotton textile, *Carbohydrate Polymers*, 91, 549- 559.
- Iguchi, Y., Ichiura, H., Kitaoka, T., & Tanaka, H. (2003). Preparation and characteristics of high performance paper containing titanium dioxide photocatalyst supported on inorganic fiber matrix. *Chemosphere*, 53(10), 1193-1199.
- 20 Kim, J., Cho, J., Seidler, P. M., Kurland, N. E., & Yadavalli, V. K. (2010). Investigations of chemical modifications of amino-terminated organic films on silicon substrates and controlled protein immobilization. *Langmuir*, 26(4), 2599-2608.
- Klemm, D., Heublein, B., Fink, H. P., & Bohn, A. (2005). Cellulose: Fascinating biopolymer and sustainable raw material. *Angewandte Chemie-International Edition*, 25 44(22), 3358-3393.
- Li, X., Chen, S. Y., Hu, W. L., Shi, S. K., Shen, W., Zhang, X., & Wang, H. P. (2009). In situ synthesis of CdS nanoparticles on bacterial cellulose nanofibers. *Carbohydrate Polymers*, 76(4), 509-512.
- Linsebigler, A.L., Lu, G.Q., & Yates, J.T. (1995). Photocatalysis on TiO<sub>2</sub> surface - principles, mechanisms, and selected results. *Chemical Reviews*, 95(3), 735-758.
- 30 Mahltig, B., Haufe, H., & Bottcher, H. (2005). Functionalisation of textiles by inorganic sol-gel coatings. *Journal of Materials Chemistry*, 15(41), 4385-4398.
- Pasternack, R.M., Amy, S.R., & Chabal, Y. J. (2008). Attachment of 3-(aminopropyl)triethoxysilane on silicon oxide surfaces: dependence on solution

- temperature. *Langmuir*, 24(22), 12963-12971.
- Pelton, R., Geng, X. L., & Brook, M. (2006). Photocatalytic paper from colloidal TiO<sub>2</sub> - fact or fantasy. *Advances in Colloid and Interface Science*, 127(1), 43-53.
- Pinto, R. J. B., Marques, Paap, Barros-Timmons, A. M., Trindade, T., & Neto, C. P. (2008). Novel SiO<sub>2</sub>/cellulose nanocomposites obtained by in situ synthesis and via polyelectrolytes assembly. *Composites Science and Technology*, 68(3-4), 1088-1093.
- 5 Ren, Y. A., Chen, M., Zhang, Y., & Wu, L. M. (2010). Fabrication of Rattle-Type TiO<sub>2</sub>/SiO<sub>2</sub> Core/Shell Particles with Both High Photoactivity and UV-Shielding Property. *Langmuir*, 26(13), 11391-11396.
- 10 Roy, D., Semsarilar, M., Guthrie, J. T., & Perrier, S. (2009). Cellulose modification by polymer grafting: a review. *Chemical Society Reviews*, 38(7), 2046-2064.
- Ryu, J., & Choi, W. (2008). Substrate-specific photocatalytic activities of TiO<sub>2</sub> and multiactivity test for water treatment application. *Environmental Science & Technology*, 42(1), 294-300.
- 15 Samuel, V., Pasricha, R., & Ravi, V. (2005). Synthesis of nanocrystalline rutile. *Ceramics International*, 31(4), 555-557.
- Song, Y.-Y., Hildebrand, H., & Schmuki, P. (2010). Optimized monolayer grafting of 3-aminopropyltriethoxysilane onto amorphous, anatase and rutile TiO<sub>2</sub>. *Surface Science*, 604(3-4), 346-353.
- 20 Ukaji, E., Furusawa, T., Sato, M., & Suzuki, N. (2007). The effect of surface modification with silane coupling agent on suppressing the photo-catalytic activity of fine TiO<sub>2</sub> particles as inorganic UV filter. *Applied Surface Science*, 254(2), 563-569.
- Vandenberg, E. T., Bertilsson, L., Liedberg, B., Uvdal, K., Erlandsson, R., Elwing, H., & Lundstrom, I. (1991). Structure of 3-aminopropyl triethoxysilane on silicon - oxide. *Journal of Colloid and Interface Science*, 147(1), 103-118.
- 25 Wold, A. (1993). Photocatalytic properties of TiO<sub>2</sub>. *Chemistry of Materials*, 5(3), 280-283.
- Youssef A. M., Kamel S., & El-Samahy M.A. (2013) Morphological and antibacterial properties of modified paper by PS nanocomposites for packaging applications, *Carbohydrate Polymers*, 98, 1166-1172.
- 30